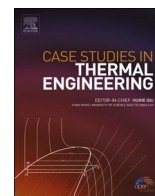




Contents lists available at ScienceDirect

## Case Studies in Thermal Engineering

journal homepage: [www.elsevier.com/locate/csite](http://www.elsevier.com/locate/csite)

## Multi-objective optimization and price performance factor evaluation of polyaniline nanofibers-palm oil nanofluids for thermal energy storage application

A.G.N. Sofiah<sup>a,\*</sup>, J. Pasupuleti<sup>a,\*\*</sup>, M. Samykano<sup>b</sup>, N.F. Sulaiman<sup>c</sup>, Z.A.C. Ramli<sup>a</sup>, R. Reji Kumar<sup>a</sup>, S. Shahabuddin<sup>d</sup>, A.K. Pandey<sup>e,f</sup>, S.K. Tiong<sup>a</sup>, S.P. Koh<sup>a</sup>

<sup>a</sup> Institute of Sustainable Energy, Universiti Tenaga Nasional (The Energy University), Jalan Ikram-Uniten, Kajang, 43000, Selangor, Malaysia

<sup>b</sup> Centre for Research in Advanced Fluid and Processes, Universiti Malaysia Pahang Al-Sultan Abdullah, Lebuhraya Tun Razak, Gambang, Kuantan 26300, Pahang, Malaysia

<sup>c</sup> Institute of Informatics and Computing in Energy, Universiti Tenaga Nasional (The Energy University), Jalan Ikram-Uniten, Kajang, 43000, Selangor, Malaysia

<sup>d</sup> Department of Science, School of Technology, Pandit Deendayal Petroleum University, Knowledge Corridor, Raisan Village, Gandhinagar, Gujarat, 382007, India

<sup>e</sup> Research Centre for Nano-Materials and Energy Technology (RCNMET), School of Science and Technology, Sunway University, No. 5, Jalan Universiti, Bandar Sunway, Petaling Jaya, 47500, Selangor Darul Ehsan, Malaysia

<sup>f</sup> Center for Transdisciplinary Research (CFTR), Saveetha University, Chennai, 602105, India

## ARTICLE INFO

Handling Editor: Huihe Qiu

## Keywords:

Density  
Viscosity  
Thermal conductivity  
Nanofluids  
Energy storage  
RSM

## ABSTRACT

The application of nanofluid in thermal energy storage technology has attracted interest among researchers in the development of novel nanofluids with high thermal conductivity behavior. Therefore, it is crucial to study the thermal physical behavior of formulated nanofluids prior to extend use in greener energy production. In this study, response surface methodology (RSM) is employed to optimize the density, viscosity and thermal conductivity behavior of formulated polyaniline-palm oil nanofluids. RSM based central composite design (CCD) is applied to extract the significant impact of temperature in the range of 30–60 °C and volume concentration of nanoadditives in the range of 0.01–0.5 vol% to the thermal physical properties of polyaniline-palm oil nanofluids and to generate empirical mathematical model for prediction purpose. Finally, the price performance factor of the studied polyaniline-palm oil nanofluids is evaluated for the first time in this research. Analysis of variance is employed to verify that the generated mathematical regression model is reliable. The formation of 45° angle line in the middle of the predicted vs actual data graph with acceptable R<sup>2</sup> of 94.43% for density model, 99.43% for viscosity model, and 94.18% for the thermal conductivity model showing an excellent agreement of both predicted and actual data and verified the reliability of the generated regression equation for response prediction. Optimal density, viscosity and thermal conductivity of polyaniline-palm oil nanofluids found to be 0.8878 g/mL, 25.8251 mPa s and 0.2877 W/mK respectively with the critical parameters for temperature and volume concentration of polyaniline are 60 °C and 0.0347 vol% respectively. The PPF evaluation shows that the higher thermal conductivity of nanofluids are not economical. The formulated polyaniline-palm oil nanofluid evaluated

\* Corresponding author.

\*\* Corresponding author.

E-mail addresses: [nurhanis.sofiah@uniten.edu.my](mailto:nurhanis.sofiah@uniten.edu.my) (A.G.N. Sofiah), [jagadeesh@uniten.edu.my](mailto:jagadeesh@uniten.edu.my) (J. Pasupuleti).

<https://doi.org/10.1016/j.csite.2023.103673>

Received 24 July 2023; Received in revised form 13 October 2023; Accepted 23 October 2023

Available online 31 October 2023

2214-157X/© 2023 The Authors. Published by Elsevier Ltd. This is an open access article under the CC BY-NC-ND license (<http://creativecommons.org/licenses/by-nc-nd/4.0/>).

properties expose the possibility of alternative advanced heat transfer fluid for thermal energy storage application due to their superior inherent qualities.

## 1. Introduction

Thermal energy storage is essential in recent technologies toward ensuring access to clean and sustainable energy. Nevertheless, there are still limitations to completely establish these instruments in greener energy production. Many scientist are vigorously trying to overcome the challenges, enhance efficiency and reduce the cost for thermal energy storage [1,2]. The utilization of nanofluid is one of the developed solutions to improve the performance of solar thermal energy storage system, as revealed by Alrowaili et al., [3]. The author and his team proposed a hybrid copper/copper oxide-water nanofluids to be serve as working fluid for solar collector instruments. According to the report, the performance of thermal energy storage was improved by 26.2% with the utilization of nanofluids showing nanofluids help to enhance the amount of energy storage.

Nanofluids are formulation of any base fluid such as water, ethylene glycol, lubricants and vegetable oils with solid nano size (<100 nm) additives [4]. Formulation of mono nanofluids involve suspension of single type nanoadditives while hybrid nanofluids generated from the dispersion of more than one type of nanoadditives [5]. The dispersion of solid nanoadditives to base fluid able to enhance its thermal conductivity properties, hence improve the performance of thermal energy storage devices. The utilization of nanofluid in thermal energy storage application has attracted interest among researchers in the development of novel nanofluids with high thermal conductivity behavior [6,7].

Recently, Bhatti et al. [8], Abdelaziz et al. [9], Akanda et al. [10], and Nabi et al. [11], reported research on nanofluid application for thermal energy storage technology. Mohamed et al. [12], employed zinc oxide nanoparticles dispersed in water to increase the performance of energy storage system by 4.8% and 6.5% compared to bare water. Bezaatpour et al. [13], utilized water base fluids to extract the effect of iron oxide nanoadditives to the performance of solar collector instruments. The author and his team reported the exergetic and energetic performance of the solar collector enhanced by 3.2% and 5.8% 5.83% respectively. According to Ding et al. [14], the titanium oxide nanoparticles suspended in water with weight percentage of 0.5, 0.7 and 1.0 wt% improved Nusselt number by approximately 18%, 29% and 41% respectively when applied to microchannels of thermal energy storage devices. Gao et al. [15], proposed nanofluid consist of hybridize graphene oxide and aluminum oxide in water base fluid to be utilize in thermal ice storage application.

The conducting polymers nanoadditives such as polyaniline nanofibers have tremendous potential to enhance the nanofluid system's thermal conductivity properties due to its excellent heat transfer capabilities [16,17]. The significant contribution of heat conduction in polyaniline nanofibers contributes by the phonon mean free path mechanism determined by nanofibers' long-distance dimension, which helps in progressive conduction of thermal energy [18,19]. However, very minimal work was reported on using conducting polymer integration in the field of heat transfer. In specific, only a few publications have been published on polyaniline nanofibers as nanoadditives in the nanofluid network. One example is Bhanvase and his team [20] that formulated polyaniline/water nanofluids in vertical helical coiled heat exchangers.

There is no communication focused on studying the effect of using oil base nanofluids on the performance of thermal energy storage. In addition, the parameter of base fluid also significantly affect the final behaviour of formulated nanofluids including density, heat capacity, rheology and heat transfer properties. Recently, oil base fluids has been explored in nanofluid research area due to its advancement in lubrication and tribology properties. However, the utilization of commercially used mineral oil can cause trouble to ecosystem [21] as 30% of these fluids will end up to the environment and resulting to aeration reduction and water infiltration. Additionally, mineral oil such as petroleum oil is running out and finding alternatives is crucial to global energy use, and is the focus of many industries [22,23]. For that reason, with the aim to provide alternative to these kind of non-renewable heat transfer oil, biodegradable and affordable vegetable oil such as palm oil is proposed in this present study. As to date, palm oil is yet to be studied extensively as the potential nano-enhanced heat transfer fluid [18,24].

Response surface methodology (RSM) is one of the approach employed to simplify laboratory work and extend researchers knowledge on the effect of various factors on the thermophysical behavior of formulated nanofluids [25,26]. Nevertheless, although there are numbers of developed mathematical model has been developed and established by previous researchers, different hypothesis were construct that lead to dissimilar outputs even though same strategies were applied in the similar behaviour. For that reason, the modelled mathematical equation for density, viscosity and heat transfer behaviour of nanofluids may overcome the challenges in the evaluation and reduce the experimental procedures for investigating its special behaviour [27,28]. As such, the present research aims to investigate the behavior of palm oil dispersed with cheap and eco-friendly conducting polymers as potential heat transfer fluid for thermal energy storage application. The formulated heat transfer fluid is later evaluated to determine the effect of composition parameters on the properties. The obtained experimental data is used to generate novel mathematical regression equation for the estimation of thermophysical properties. The price performance factor is also calculate in order to investigate the economic status of the studied nanofluids as formulated parameters.

## 2. Methodology

The research project starts with the synthesis procedure of polyaniline nanofibers, prior to formulation of nanofluids. Then, the research project was extended to study the density, viscosity, and thermal conductivity of the prepared polyaniline-palm oil nanofluids with respect to the volume concentration of polyaniline nanofibers and applied temperature. The research's final division is developing

the mathematical model of thermophysical properties of prepared nanofluids by using the RSM method.

### 2.1. Materials and resources

Aniline(Merck), Ammonium peroxydisulphate(Merck), Hydrochloric acid(Merck), Acetone(Merck) and Methanol(Merck) were used to synthesize the polyaniline nanofibers. Distilled water was employed throughout the entire work. The laboratory grade of palm oil supplied by the Research and Development Centre of Sime Darby Plantation, Malaysia, was used in the study.

### 2.2. Synthesis of polyaniline nanofibers

In situ oxidative polymerization approach was employed to synthesize polyaniline nanofibers. An oxidant solution consist of 0.0268 mol ammonium persulphate and 35 ml 1 M hydrochloric acid was added slowly to the mixture of 0.0215 mol aniline and 30 ml 1 M hydrochloric acid. The oxidative polymerization reaction of the mixture take place for 3 h with continuous stirring on the hot plate at constant temperature of 25 °C. The collection of precipitate via centrifuge filtration method was done prior to washing process of the supernatant by using 0.5 M hydrochloric acid and distilled water until the obtained product become neutral (pH = 7) and colorless. Then, the obtained product is washed with a 1:1 (v/v) mix solution of acetone and methanol to remove all unreacted precursors. The final precipitate left overnight in the laboratory vacuum dryer at constant temperature of 60 °C with 100 mbar vacuum power. Finally, the polyaniline nanofibers was crashed by using mortar and pestle until the polymers become very fine powder. Fig. 1 illustrates the step in the synthesis of polyaniline nanofibers from aniline into powder form of nanoadditives.

The morphology, particle size, and structure shape characterization at the nanoscale were evaluated via Philips Tecnai F20 Transmission Electron Microscope (TEM) approach as displayed in Fig. 2(a). The TEM image clearly shows the nano-sized fiber-like

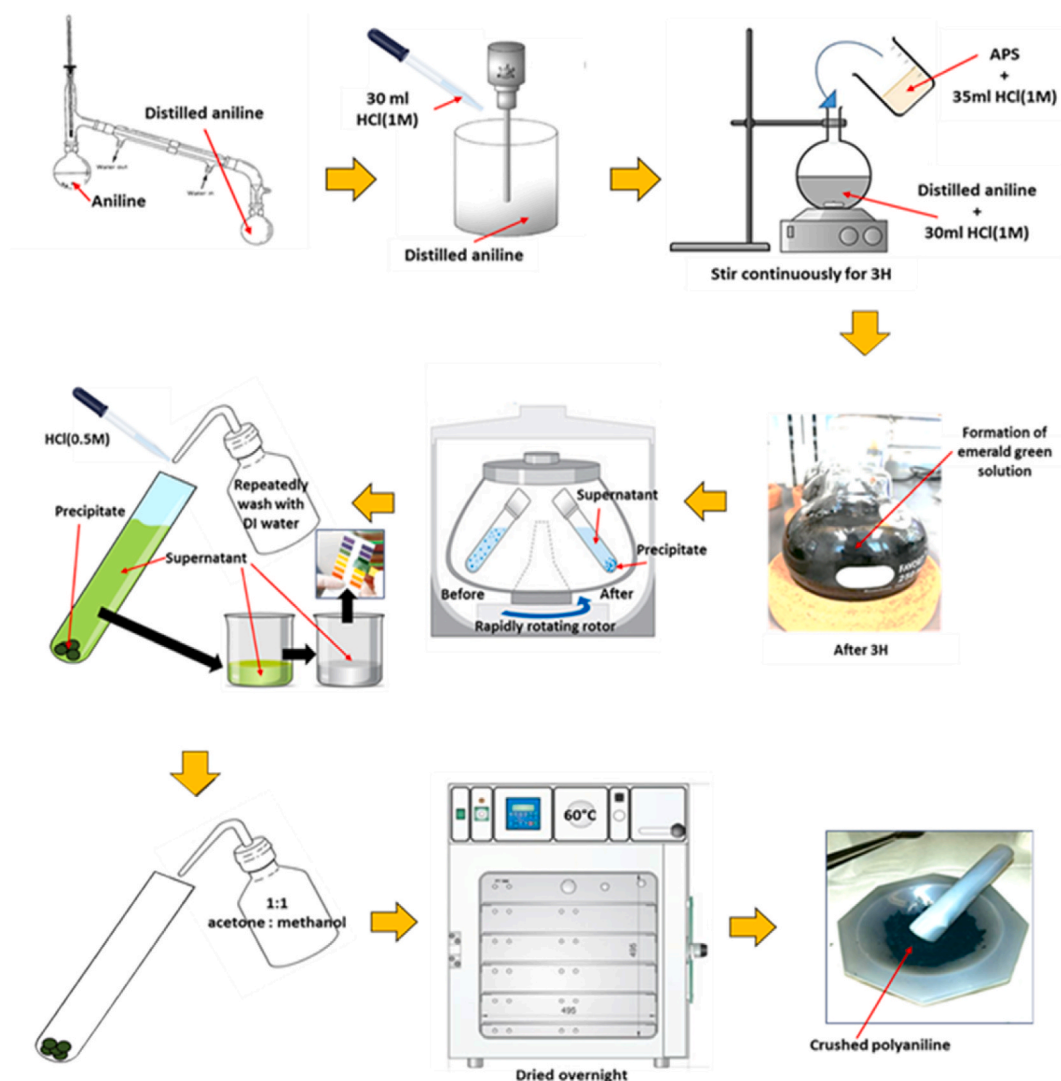


Fig. 1. Illustration of polyaniline nanofibers synthesis method.

structure with a large aspect ratio of polyaniline nanofibers. Many researchers suggested that nanofluids' significant factor that affects the heat transfer ability is the aspect ratio (major axis: minor axis) of nanoadditives [19]. The structural and phase identification of polyaniline nanofibers was done by XRD, Bruker Advance 8 with CuK $\alpha$  radiation (wavelength,  $\lambda = 1.5406 \text{ \AA}$ ) generated at an operating voltage and current of 40 kV and 30 mA, respectively. The XRD spectrum of polyaniline nanofibers in Fig. 2(b) presents multiple diffraction peaks suggesting polyaniline nanofibers' polycrystalline behavior.

### 2.3. Preparation of polyaniline nanofibers-palm oil nanofluids

A two-step approach was used to prepare the nanofluids. The nanofluids were formulated with different volume concentration of 0.01-0.5 vol% in 100 ml of palm oil. The weight of polyaniline was determined and calculated using the law of mixture Equation (1):

$$\phi = \frac{\left[ \frac{w_p}{\rho_p} \right]}{\left[ \frac{w_p}{\rho_p} + \frac{w_{bf}}{\rho_{bf}} \right]} \quad (1)$$

Polyaniline nanofibers were weighed via a precision electronic balance. The nanofibers were suspended in palm oil and the suspension was sonicated using a probe sonicator (FS-1200 N, frequency: 50 kHz, power output: 1200 W, 25 mm probe) at 60% amplitude for 2 h to ensure the homogeneous and stability of the nanofluids. To optimize the sonication time, we conducted a systematic investigation of the nanofluid at various sonication durations. The dynamic light scattering (DLS) approach allowed us to monitor the size distribution of the nanoparticles in real-time. Based on our comprehensive DLS analysis and observations, we confidently set the sonication time to 2 h as the optimized condition for our nanofluid preparation. During the sonication procedure, the sample temperature was maintained under 40 °C and placed inside the ice bath as displayed in Fig. 3. These parameters were kept constant for all the prepared samples.

### 2.4. Density evaluation of polyaniline-palm oil nanofluids

The density of prepared polyaniline-palm oil nanofluids evaluated via density meter from Anton Paar DMA 4500 at a temperature of 30–60 °C, with an error of 0.001 g/ml. Before and after the measurement sequence, it is essential to calibrate the instrument by measuring the density of water at ambient temperature, as shown in Table S1 (Supplementary information). Also, it is significant to clean and rinse the oscillating U-tube to ensure accurate measurement. The contaminated oscillating tube may cause the density value of water will start to vary. For each sample, five (5) measurements were taken at varying temperatures.

### 2.5. Viscosity evaluation of polyaniline-palm oil nanofluids

Rheological properties of the nanofluids were analyzed via Anton Paar MCR 92 Rheometer with a standard uncertainty of  $\pm 1\%$ . A concentric cylinder (CC39), with a volume sample of 60 ml is required for such measuring geometry. The experimental data were recorded and analyzed using Rheo-compass software equipped with the rheometer. The measuring system were calibrated with distilled water at ambient temperature, and the obtained data were then compared with the literature source, as shown in Fig. S1 (Supplementary information). T-ramp measurement was conducted at a temperature range of 30–60 °C (maintained with Peltier device, C-PTD200 SN82169343) at a fixed shear rate of  $10 \text{ s}^{-1}$ .

### 2.6. Thermal conductivity properties evaluation of polyaniline- palm oil nanofluids

Thermal conductivity properties of nanofluids was evaluated by using hot wire principle thermal analyzer from TEMPOS-Meter Environment, USA. The instrument consist of 60 mm length and 1.3 mm diameter sensor needles (KS-3) with high sensitivity that

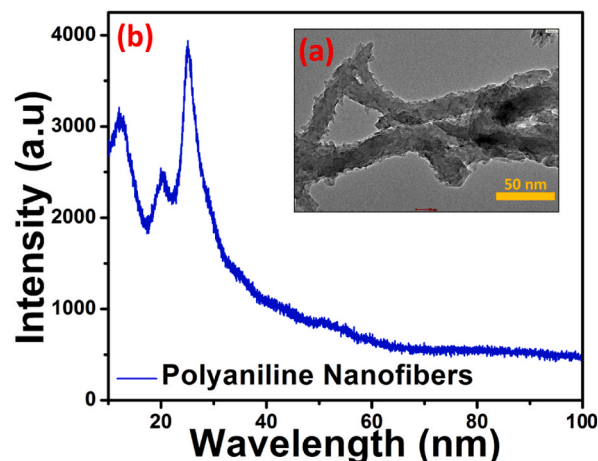


Fig. 2. TEM and XRD analysis of polyaniline nanofibers.



Fig. 3. Illustration of polyaniline-palm oil nanofluids formulation method.

serve as heating elements and thermostat. Before measurements, the measuring system was validated by measuring the thermal conductivity properties of provided glycerine from the instrument’s supplier. The verification outputs were then compared with meter group Inc. USA reading (0.282W/m.K) and found to have a great agreement with the instrumental accuracy measurements, as shown in Table S2 (Supplementary information). In order to keep a constant temperature and extract accurate data, the fresh formulated nanofluids were placed inside the laboratory water bath with the set temperature (30 °C, 40 °C, 50 °C, and 60 °C). The uncertainty of the thermal conductivity measurement was estimated to be lower than 3%.

2.7. Response surface methodology

The response surface method (RSM) is used to develop a mathematical equation from the obtained experimental data. The RSM can generate the optimal parameter value based on the mathematical and statistical technique. The effect of temperature factor and volume concentration factor on specific responses of density, viscosity, and thermal conductivity (as presented in Table 1) was estimated via central composite design (CCD). The calculation of a full quadratic mathematical regression model was generated via Minitab 19 software by examining the regression coefficient, analysis of variance (ANOVA), and diagnostic of the model graphs. The fit quality of the developed mathematical equation model was analyzed to investigate the developed model’s reliability. The basic mathematical equation model in RSM is based on a linear function and is presented as follows:

$$Y = \beta_0 + \sum_{i=1}^n \beta_i x_i + \sum_{i=1}^n \beta_{ii} x_i^2 + \sum_{i=1}^n \sum_{j=1}^n \beta_{ij} x_i x_j + \epsilon^1 \tag{2}$$

where,  $Y$  is the predicted response,  $n$  is the number of variables,  $\beta_0$  is the intercept,  $\beta_i$  represents the first model of linear parameters,  $\beta_{ii}$  the second-order (quadratic) coefficient,  $\beta_{ij}$  the coefficient of an interaction effect,  $x_i$  and  $x_j$  represents variables and  $\epsilon$  is the residual associated to the experiments, and the second-order model This model may cover a variety of functions.

The relationship between continuous variables and response variables is expressed in a mathematical regression equation. A systematic comparison was conducted between the experimental and prediction data and the results obtained from the regression comparison in order to determine the validity of the generated regression model. The influence of volume concentration and applied temperature on density, viscosity and thermal conductivity properties is studied for about 28 experiments, including base fluids at different temperature. Palm oil’s measurements of density, viscosity, and thermal conductivity align closely with the values reported in the literature, indicating a high degree of agreement [29,30]. Table 2 summarizes the layout design with the findings from the experimental data.

Table 1  
Levels of factors.

| Type of Factors    | Factors              | -1   | +1  |
|--------------------|----------------------|------|-----|
| Continuous factors | Temperature          | 30   | 60  |
|                    | Volume concentration | 0.01 | 0.5 |

## 2.8. Price performance factor evaluation

The economic analysis was evaluated by using price performance factor (PPF) equation [31–33] as presented in Equation (3):

$$PPF = \frac{RTC}{\text{price} \left( \frac{\$}{\text{lit}} \right)} \quad (3)$$

The obtained data from thermal conductivity measurement were further used for relative thermal conductivity calculation as summarized in Table S3 (supplementary information). The PPF was analyzed by calculating the cost of formulation each liter of polyaniline-palm oil nanofluids at different volume concentration of polyaniline nanofibers. The preparation expenses of the studied nanofluids was tabulated in Table S4 (supplementary information).

## 3. Results and analysis

### 3.1. Influence of independent variables on responses for density of polyaniline-palm oil nanofluids

The purpose of regression study is to check the best-fitted regression from the obtained experimental data in the form of mathematical regression model as proposed in Equation (4). Fig. 4(a) presents normal plot of residual for density of polyaniline-palm oil data. The generated graph displays all data plotted within one straight line, validating that the value of residual is having appropriate standard error terms. The comparison of estimated density by developed mathematical model with the present experimental data is revealed in Fig. 4(b). The formation of 45° angle red line in the middle of the graph that align with all the plotted data showing an excellent agreement of both predicted and actual data and verified the reliability of the generated regression equation for response prediction.

Table 3 summarized informative contribution of every single generated term in the developed mathematical model. F-values and P-values represents the ability of the proposed model and separation values of relevant and irrelevant relationship boundaries respectively [34]. A high value of 98.39 indicates that the proposed model is in excellent agreement with the actual experimental data. Less than 0.05 of P-value reflects as an essential correlation parameters while more than 0.1 P-value indicates that the parameters has no significant impact. Analysis of Variance generates the assurance of R<sup>2</sup> and standard deviation which represent the reliability of the proposed equation. 0.9443 and 0.0023065 of R<sup>2</sup> and standard deviation values respectively verify that 94.43% of the total variation can be correspondent by the proposed regression equation. Besides, the 91.78% and 93.47% of predicted R<sup>2</sup> and adjusted R<sup>2</sup> respectively indicates the reliable agreement.

$$\rho_{nf} = 0.92618 + 0.0242\varnothing - 0.0729\varnothing^2 + 0.000758T\varnothing \quad (4)$$

Fig. 5 present the effect of studied factors on the density of polyaniline-palm oil nanofluids via 2D contour plot. The 2D contour plot indicates volume concentration has a significant influence on the density of polyaniline-palm oil nanofluids. The graph clearly

**Table 2**  
Design of experiments and its findings.

| Std | Temperature (°C) | Volume Concentration (vol%) | Density (g/ml) | Viscosity (mPa.s) | Thermal Conductivity (W/m.K) |
|-----|------------------|-----------------------------|----------------|-------------------|------------------------------|
| 1   | 30               | 0                           | 0.905          | 68.968            | 0.115                        |
| 2   | 40               | 0                           | 0.898          | 54.359            | 0.197                        |
| 3   | 50               | 0                           | 0.892          | 36.143            | 0.222                        |
| 4   | 60               | 0                           | 0.885          | 25.614            | 0.271                        |
| 5   | 30               | 0.01                        | 0.905          | 66.093            | 0.124                        |
| 6   | 40               | 0.01                        | 0.898          | 53.763            | 0.198                        |
| 7   | 50               | 0.01                        | 0.892          | 36.127            | 0.223                        |
| 8   | 60               | 0.01                        | 0.885          | 25.467            | 0.269                        |
| 9   | 30               | 0.03                        | 0.905          | 67.028            | 0.136                        |
| 10  | 40               | 0.03                        | 0.899          | 53.991            | 0.201                        |
| 11  | 50               | 0.03                        | 0.892          | 37.818            | 0.231                        |
| 12  | 60               | 0.03                        | 0.885          | 26.462            | 0.270                        |
| 13  | 30               | 0.05                        | 0.906          | 67.981            | 0.148                        |
| 14  | 40               | 0.05                        | 0.899          | 54.299            | 0.218                        |
| 15  | 50               | 0.05                        | 0.892          | 38.103            | 0.244                        |
| 16  | 60               | 0.05                        | 0.885          | 26.781            | 0.271                        |
| 17  | 30               | 0.1                         | 0.909          | 76.928            | 0.215                        |
| 18  | 40               | 0.1                         | 0.905          | 59.182            | 0.261                        |
| 19  | 50               | 0.1                         | 0.902          | 43.231            | 0.310                        |
| 20  | 60               | 0.1                         | 0.900          | 27.997            | 0.379                        |
| 21  | 30               | 0.3                         | 0.910          | 78.567            | 0.228                        |
| 22  | 40               | 0.3                         | 0.906          | 59.673            | 0.272                        |
| 23  | 50               | 0.3                         | 0.903          | 44.989            | 0.320                        |
| 24  | 60               | 0.3                         | 0.899          | 29.093            | 0.386                        |
| 25  | 30               | 0.5                         | 0.910          | 80.523            | 0.233                        |
| 26  | 40               | 0.5                         | 0.907          | 62.678            | 0.286                        |
| 27  | 50               | 0.5                         | 0.904          | 46.728            | 0.330                        |
| 28  | 60               | 0.5                         | 0.901          | 31.879            | 0.387                        |

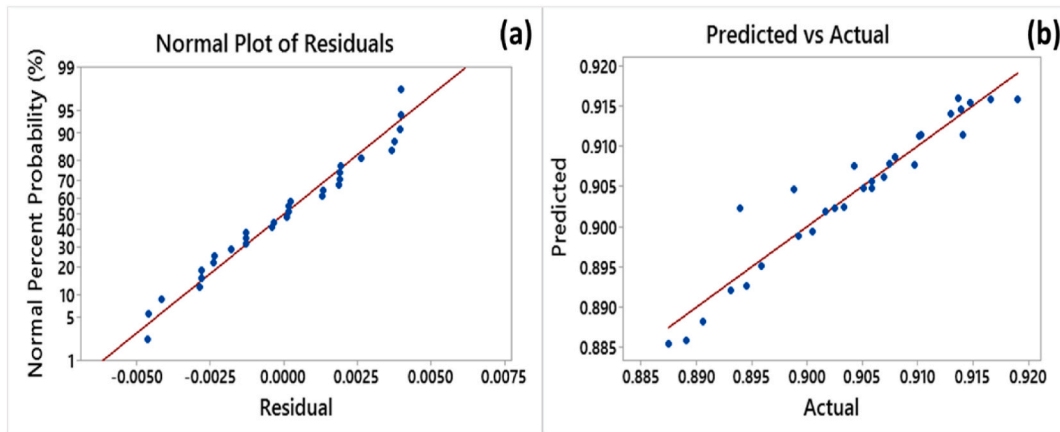


Fig. 4. (a) Normal plot of residual and (b) Predicted vs. actual plot on density of polyaniline-palm oil nanofluids.

**Table 3**  
Analysis of variance for density of polyaniline-palm oil nanofluids.

| Parameter         | Sum of square | Contribution | Mean square | F value | P-value |                 |
|-------------------|---------------|--------------|-------------|---------|---------|-----------------|
| Model             | 0.002617      | 94.43%       | 0.000523    | 98.39   | 0.000   | significant     |
| Linear            | 0.001383      | 87.02%       | 0.000691    | 129.94  | 0.000   | significant     |
| Temp              | 0.001041      | 72.69%       | 0.001041    | 195.70  | 0.000   | significant     |
| vol%              | 0.000341      | 14.33%       | 0.000341    | 64.18   | 0.000   | significant     |
| Square            | 0.000083      | 2.99%        | 0.000041    | 7.78    | 0.002   | significant     |
| vol%*vol%         | 0.000080      | 2.88%        | 0.000123    | 15.03   | 0.001   | significant     |
| 2-way interaction | 0.000123      | 4.43%        | 0.000123    | 23.08   | 0.000   | significant     |
| Temp*vol%         | 0.000123      | 4.43%        | 0.000005    | 23.08   | 0.000   | significant     |
| Residual          | 0.000154      | 5.57%        |             |         |         |                 |
| Lack of fit       | 0.000154      | 5.57%        |             |         | 0.1766  | Not significant |
| Pure error        | 0.00          |              |             |         |         |                 |

displayed the increasing of the volume concentration of polyaniline nanofibers increases the density of nanofluids. By contrast, by increasing the nanofluid temperature, density was found to decrease and revealed that nanofluid temperature contributes high impact on nanofluid density. Also, there are too many theories about the reasons of density increases by temperature increment. The 3D surface plot in Fig. 6 also showed a consistent trend as in the 2D contour plot, and the apparent peak for temperature and volume

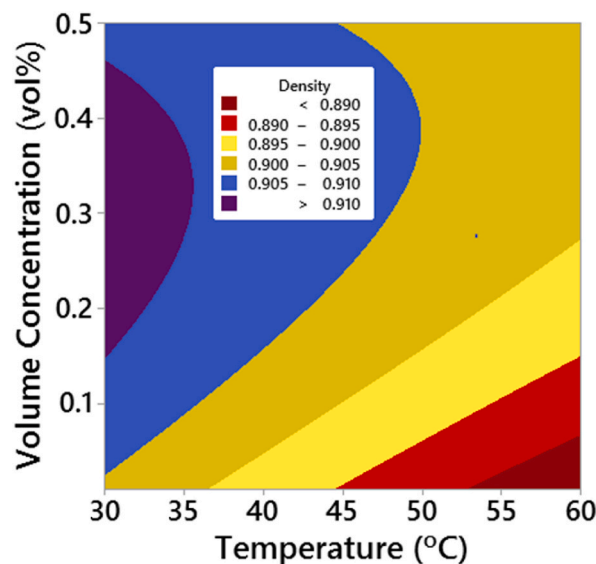


Fig. 5. Interaction effect of temperature and nanoparticles volume concentration on density response: contour plot.

concentration factors is an optimum achievement for the density response.

Pareto chart was employed to observe the significant of each standardized effect. The density response of polyaniline-palm oil nanofluids is presented in Fig. 7. The obtained density data divided into segments in order to generate Pareto chart. The relative magnitude and statistical effect of primary factors (A and B) and their interactions (interactions AB), the Pareto chart also presents the relative factors of the significant effects. Segment that has a significant impact will exceed the red reference line (2.05 standardized effect). Therefore, from the obtained Pareto chart, can be concluded that segment A (temperature), B (volume concentration), AB (temperature\*volume concentration) and BB (volume concentration\*volume concentration) are significant, but the interaction AA (temperature\*temperature) are not significant for the density response of the present study. The most significant impact is segment A, showing that the applied temperature significantly influence the density response.

The RSM plotted graph for density of polyaniline-palm oil residual plots demonstrates the reliability of the empirical mathematical equation's prediction with a zero mean error. In Fig. 8, top left plot presents the normal probability graph that indicates the error terms are typical. The plotted points are clustered on the red straight line of the graph validate that the error terms are relatively normal and normality prediction is verified. The top right illustrate versus fits plot consist of error terms plotted against the fitted values. The plotted points appear to be evenly scattered for both at the top and bottom of the reference line. The bottom right of residual vs observation plotted graph indicates the relationship between the response and error and correspond to the versus fits plot.

### 3.2. Influence of independent variables on responses for viscosity of polyaniline-palm oil nanofluids

The empirical experiments on polyaniline-palm oil nanofluids' viscosity with studied parameters of volume concentration and temperature have been done via RSM. Table 4 listed the importance and contribution of each generated parameters. The mathematical regression equation that has been developed via RSM for estimation of viscosity of polyaniline-palm oil nanofluids is presented in Equation (5). Fig. 9(a) presents normal plot of residual for density of polyaniline-palm oil data. The generated graph displays all data plotted within one straight line, validating that the value of residual is having appropriate standard error terms. The comparison of estimated density by developed mathematical model with the present experimental data is revealed in Fig. 9(b). The formation of 45° angle red line in the middle of the graph that align with all the plotted data showing an excellent agreement of both predicted and actual data and verified the reliability of the generated regression equation for response prediction.

$$\mu_{nf} = 135.51 - 2.6458T + 50.68\varnothing + 0.013886T^2 - 32.0\varnothing^2 - 0.3403T\varnothing \quad (5)$$

In the analysis of variance for viscosity of polyaniline-palm oil nanofluids, 0.9943 of  $R^2$  and value verify that 99.43% of the total variation can be correspondent by the proposed regression equation. The regression model's importance is implied by the high F-value (1459.34). The models corresponding P-values of <0.05 denote the statistical significance of model terms, and the impacts of model terms with P-values of higher than 0.05 are unimportant. Additionally, the predicted R square and adjusted R square values of 99.25% and 99.36% are in reliable agreement. Therefore, the ANOVA implies that this developed mathematical equation model can be used to examine the actual data in the design space.

Figs. 10 and 11 present the impact of studied parameters on nanofluids' viscosity in 2D contour plot and 3D surface plot, respectively. Fig. 11 shows nanoadditive's volume concentration has a significant influence on the viscosity of polyaniline-palm oil nanofluids. The graph clearly showed, at the higher amount of polyaniline nanofibers, viscosity of nanofluid increase. By contrast, by increasing nanofluid's temperature, the nanofluids become less viscous suggested that high concentration of polyaniline significantly enhance the viscosity of studied nanofluids. The 3D chart found to have excellent agreement as in the 2D contour graph and the apparent peak for temperature and volume concentration factors is an optimum achievement for the viscosity response.

The highest viscosity is achieved at the temperature of 30 °C and when the volume concentration of polyaniline is high (refer upper left corner of the 3D plot). Volume concentration of polyaniline and applied temperature interact to provide significant influences to the viscosity of polyaniline-palm oil nanofluids. The 3D plot indicates that the highest temperature of 60 °C and the lowest volume

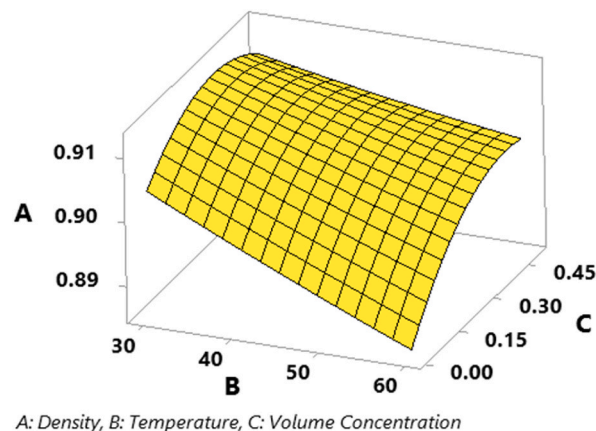


Fig. 6. Interaction effect of temperature and nanoparticles volume concentration on density response: 3D plot.

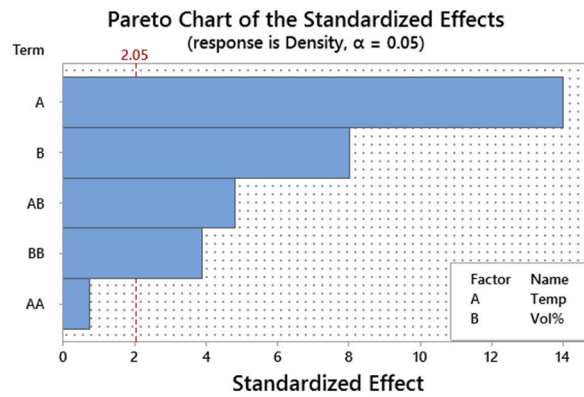


Fig. 7. Pareto chart of the standardized effect for density of polyaniline-palm oil nanofluids.

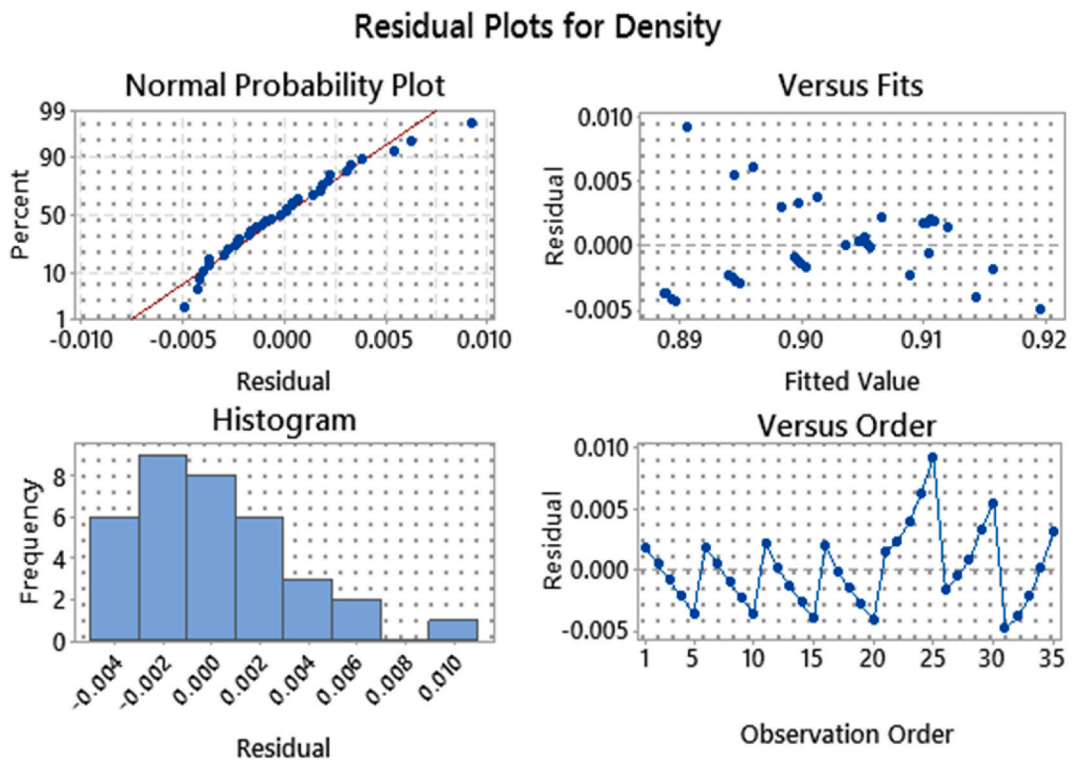


Fig. 8. Residual plot of density for polyaniline-palm oil nanofluids.

concentration of polyaniline nanofibers of 0.01 vol% exhibit minimum viscosity of polyaniline-palm oil nanofluids in value range of <30. Theoretically, the less viscous nanofluids effect from the high applied temperature is influence by the hydrodynamic interaction between solid additives as the disturbance of the base fluid around one particle interacts with that around other particles at higher volume concentrations [35,36]. Besides, at ambient condition, the minimization of fluid layers movement occur donated from the room temperature solid additives [37,38]. However, this mechanism changed at higher temperature due to the weaker Van der Waals forces among the solid atoms causes them to move freely in the base fluids resulting to the lower viscosity of nanofluids [39,40].

Fig. 12 presents a Pareto chart of the standardized impacts of viscosity for polyaniline-palm oil nanofluids. Segments B(temperature), BB(temperature\*temperature), A(volume concentration), and AB(volume concentration\*temperature) that exceed the red reference line with value of 2.02 indicates their significant effect to the viscosity properties of nanofluids. The segment of AA(volume concentration\*volume concentration) that is slightly exceed the reference line indicates the less importance of this factors to the viscosity of studied nanofluid. The most significant impact is segment B showing that the applied temperature significantly influence the viscosity of polyaniline-palm oil nanofluids.

The residual plots of viscosity for polyaniline-palm oil nanofluids in Fig. 13 showing a zero value of mean error validate the

**Table 4**  
Analysis of variance for viscosity of polyaniline-palm oil nanofluids.

| Parameter         | Sum of square | Contribution | Mean square | F value | P-value |                 |
|-------------------|---------------|--------------|-------------|---------|---------|-----------------|
| Model             | 22562.7       | 99.43%       | 4512.5      | 1459.34 | 0.000   | significant     |
| Linear            | 20505.3       | 90.36%       | 8742.9      | 2627.41 | 0.000   | significant     |
| Temp              | 240.8         | 1.06%        | 225.0       | 72.77   | 0.000   | significant     |
| vol%              | 20264.5       | 89.3%        | 17260.8     | 5582.05 | 0.000   | significant     |
| Square            | 1965.0        | 8.66%        | 982.5       | 317.73  | 0.000   | significant     |
| Temp*Temp         | 21.3          | 0.09%        | 21.3        | 6.88    | 0.012   | significant     |
| vol%*vol%         | 1943.7        | 8.57%        | 1943.7      | 628.59  | 0.000   | significant     |
| 2-way interaction | 92.5          | 0.41%        | 92.5        | 29.91   | 0.000   | significant     |
| Temp*vol%         | 92.5          | 0.41%        | 92.5        | 29.91   | 0.000   | significant     |
| Residual          | 129.9         | 0.57%        |             |         |         |                 |
| Lack of fit       | 129.9         | 0.57%        |             |         | 0.244   | Not significant |
| Pure error        | 0.00          |              |             |         |         |                 |

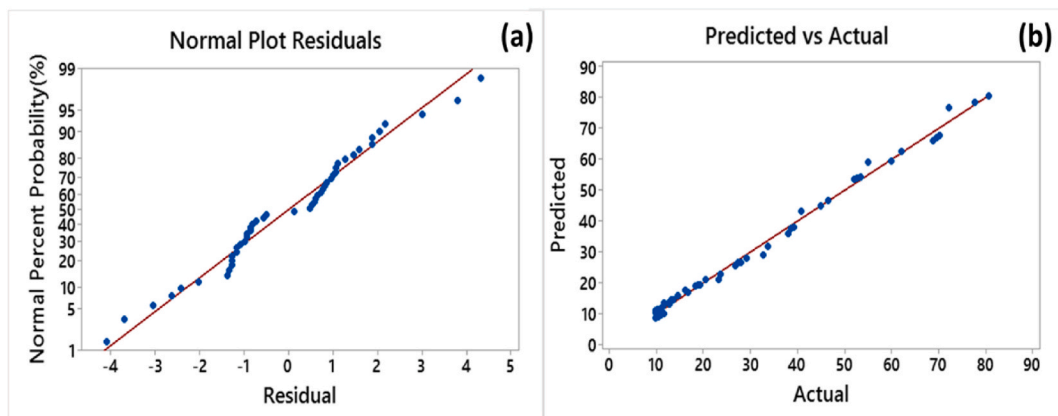


Fig. 9. (a) Normal plot of residual and (b) Predicted vs. actual plot on viscosity of polyaniline-palm oil nanofluids.

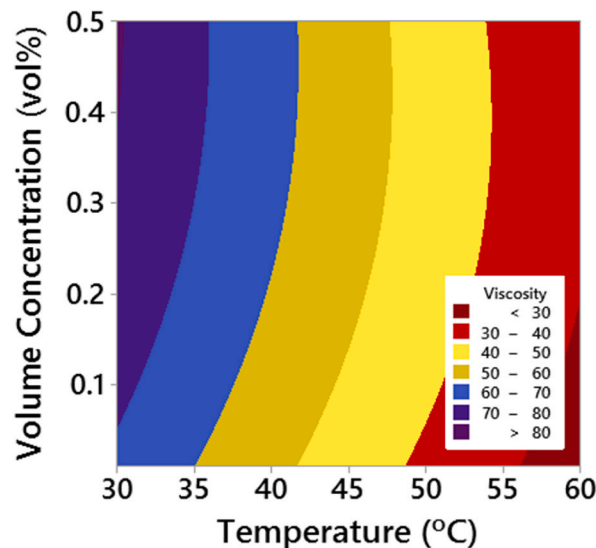
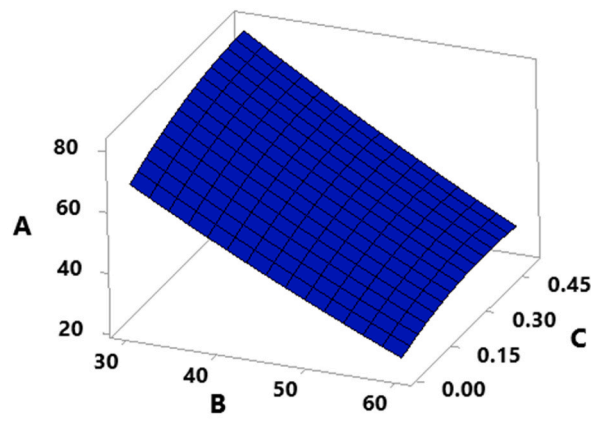


Fig. 10. Interaction effect of temperature and nanoparticles volume concentration on viscosity response: contour plot.

correctness of the mathematical regression equation’s predictions. The top left of normal probability graph verifies normal error terms. On the plotted graph, the data points found to be clusters align with the red straight line showing that the error terms are relatively normal. The top right illustrate versus fits plot consist of error terms plotted against the fitted values. The plotted points appear to be evenly scattered for both at the top and bottom of the reference line. The bottom right of residual vs observation plotted graph indicates



A: Viscosity, B: Temperature, C: Volume Concentration

Fig. 11. Interaction effect of temperature and nanoparticles volume concentration on viscosity response: 3D plot.

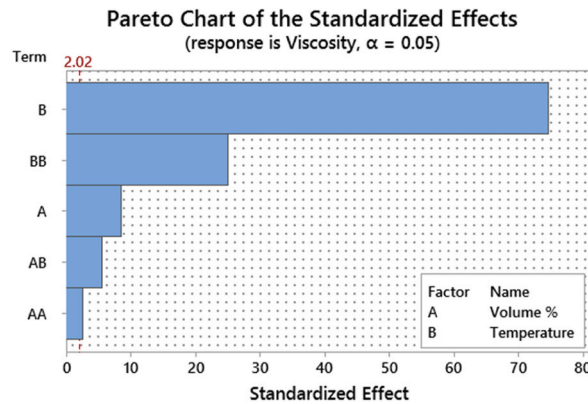


Fig. 12. Pareto chart of the standardized effect for viscosity of polyaniline-palm oil nanofluids.

the relationship between the response and error and correspond to the versus fits plot.

### 3.3. Influence of independent variables on responses for thermal conductivity properties of polyaniline-palm oil nanofluids

In the context of mathematical regression model, no equation has been developed in the literature for thermal physical properties of polyaniline-palm oil nanofluids with respect to studied parameters. Equation (6) has been proposed to estimate the heat transfer behaviour of these nanofluids at any temperature and nanoadditives’s volume concentration. The normal plot of residuals in Fig. 14(a) presents normal plot of residual for thermal conductivity of polyaniline-palm oil data. The generated graph displays all data plotted within one straight line, validating that the value of residual is having appropriate standard error terms. The comparison of estimated thermal conductivity by developed mathematical model with the present experimental data is revealed in Fig. 14(b). The formation of 45° angle red line in the middle of the graph that align with all the plotted data showing an excellent agreement of both predicted and actual data and verified the reliability of the generated regression equation for response prediction.

Table 5 listed informative contribution of every single generated term in the developed mathematical model. The generated empirical model for heat transfer properties of polyaniline-palm oil nanofluids is manifested based on the temperature and volume concentration of nanoadditives. 0.9418 of R<sup>2</sup> verify that 94.18% of the total variation can be correspondent by the proposed regression equation. Besides, the 92.28% and 93.21% of predicted R<sup>2</sup> and adjusted R<sup>2</sup> respectively indicates the reliable agreement. Therefore, the ANOVA implies that this developed mathematical equation model can be used to examine the actual data in the design space

$$k_{nf} = -0.0419 + 0.00629T + 0.641\varnothing - 0.000019T^2 - 0.854\varnothing^2 - 0.00011T\varnothing \tag{6}$$

Figs. 15 and 16 present 2D contour plot and 3D surface plot respectively that report the effect of temperature and amount of polyaniline dispersed in palm oil to the specific response of studied nanofluids. Fig. 16 clearly displays the significant impact of volume concentration of polyaniline to the heat transfer properties of polyaniline-palm oil nanofluids. Increasing dispersion amount of polyaniline nanofibers and temperature improves the fluid’s thermal conductivity behavior. At the highest temperature of 60 °C, the most enhanced thermal conductivity properties of polyaniline-palm oil nanofluids achieved with the reading approximately about 0.4 W/m.

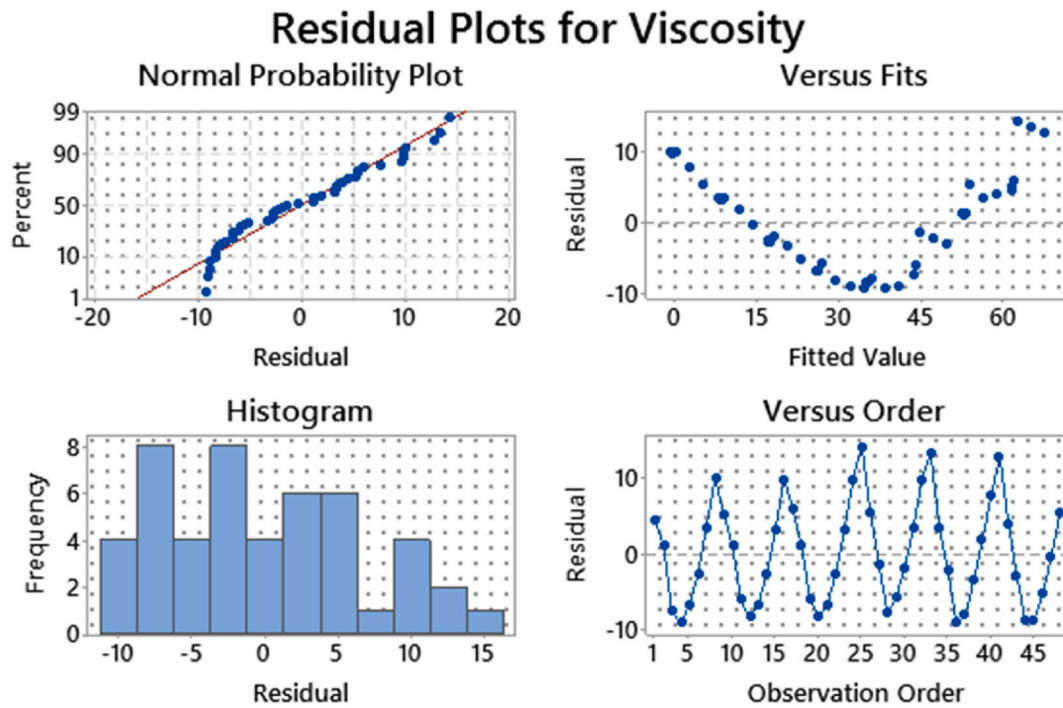


Fig. 13. Residual plot of viscosity for polyaniline-palm oil nanofluids.

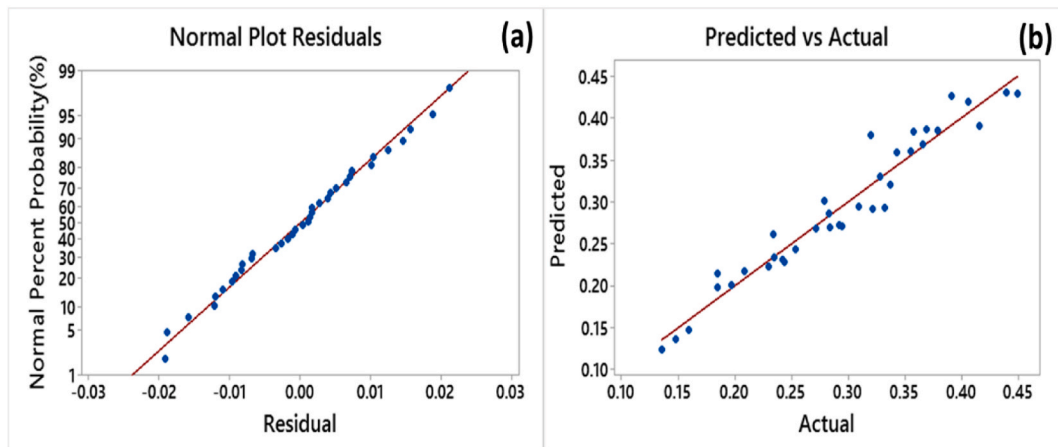


Fig. 14. (a) Normal plot of residual and (b) Predicted vs. actual plot on thermal conductivity of polyaniline-palm oil nanofluids.

**Table 5**  
Analysis of variance for thermal conductivity of polyaniline-palm oil nanofluids.

| Parameter   | Sum of square | Contribution | Mean square | F value | P-value |                 |
|-------------|---------------|--------------|-------------|---------|---------|-----------------|
| Model       | 0.241554      | 94.18%       | 0.048311    | 97.08   | 0.000   | significant     |
| Linear      | 0.229357      | 89.42%       | 0.093609    | 188.10  | 0.000   | significant     |
| Temp        | 0.179581      | 70.02%       | 0.142363    | 286.07  | 0.000   | significant     |
| vol%        | 0.049776      | 19.41%       | 0.044855    | 90.13   | 0.000   | significant     |
| Square      | 0.012193      | 4.75%        | 0.006097    | 12.25   | 0.000   | significant     |
| vol%*vol%   | 0.011351      | 4.43%        | 0.011351    | 22.81   | 0.000   | significant     |
| Residual    | 0.014929      | 5.82%        |             |         |         |                 |
| Lack of fit | 0.014929      | 5.82%        |             |         | 0.331   | Not significant |
| Pure error  | 0.00          |              |             |         |         |                 |

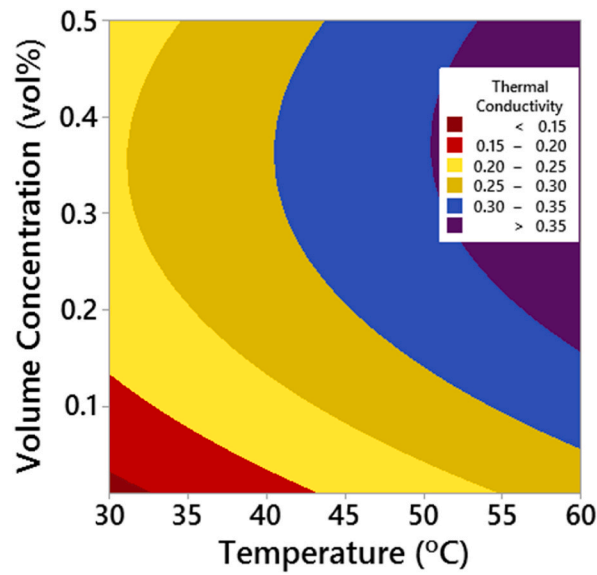


Fig. 15. Interaction effect of temperature and nanoparticles volume concentration on thermal conductivity response: contour plot.

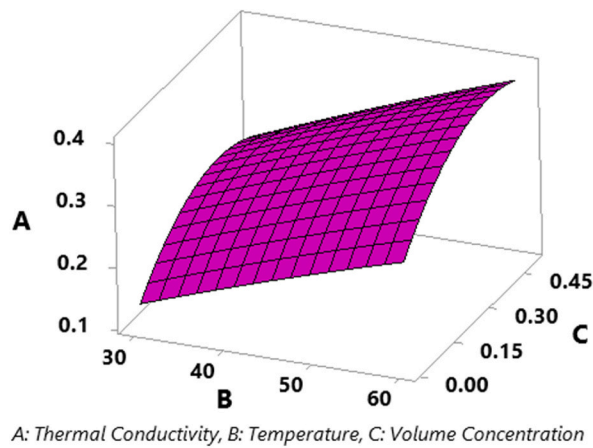


Fig. 16. Interaction effect of temperature and nanoparticles volume concentration on thermal conductivity response: 3D plot.

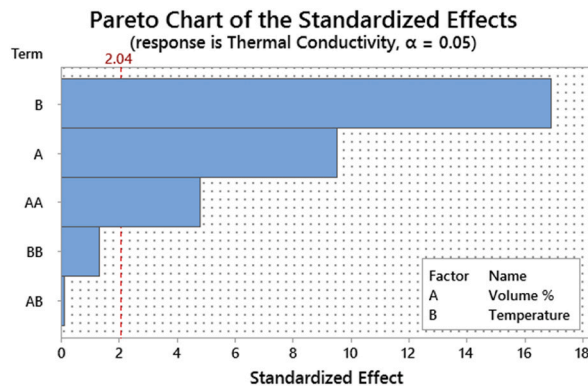


Fig. 17. Pareto chart Pareto chart of the standardized effect for thermal conductivity of polyaniline-palm oil nanofluids.

K with volume concentration of 0.5vol. This revealed that the higher amount of nanoadditives and nanofluid temperature contribute an enhancement of the thermal conductivity of nanofluid.

The 3D surface plot also displayed a consistent trend as in the 2D contour plot, and the apparent peak for for temperature and volume concentration factors is an optimum achievement for the thermal conductivity response. From the upper right corner of the 3D plot indicates that the highest temperature and volume concentration of polyaniline nanofibers, maximum thermal conductivity if nanofluid is obtained. The reducing in thermal conductivity properties of nanofluid can be clearly seen as the volume concentration of nanoadditives decreases with the thermal conductivity value in the range of 0.15–0.2 at lower temperature of 30–40 °C. The 3D surface plot reveals that the quadratic model is fitted with polyaniline-palm oil nanofluid thermal conductivity model. Higher amount of polyaniline dispersion in palm oil cause the arrangement of solid atoms to become closer resulting to the high rate of heat conductivity among them due to Brownian motion mechanism [41,42]. Besides, the enhancement in thermal conductivity properties also contribute by the molecular layering effect formed at the solid-liquid interphase [43,44].

Fig. 17 presents a Pareto chart of the standardized impacts of thermal conductivity for polyaniline-palm oil nanofluids. Segments B (temperature), A(volume concentration), and AA(volume concentration\*volume concentration) hat exceed the red reference line with value of 2.04 indicates their significant effect to the thermal conductivity properties of nanofluids. The segment of BB(temperature\*temperature) and AB(volume concentration\*temperature) that is located before the reference line indicates this factors has no significant impact to the thermal conductivity properties of studied nanofluid. The most significant impact is segment B showing that the applied temperature significantly influence the heat transfer behaviour of polyaniline-palm oil nanofluids.

The response surface methodology charts of residual plots for heat transfer properties of polyaniline-palm oil nanofluids in Fig. 18 illustrates the validity of the mathematical regression equation's prediction with zero mean error value. The plotted point found to be clustered align with the straight line of the graph verify that the error terms are relatively normal. This can concluded that the normality prediction of the modeling is verified. The top right illustrate versus fits plot consist of error terms plotted against the fitted values. The plotted points appear to be evenly scattered for both at the top and bottom of the reference line. The bottom right of residual vs observation plotted graph indicates the relationship between the response and error and correspond to the versus fits plot.

#### 3.4. Multi-objective optimization of density, viscosity and thermal conductivity of polyaniline-palm oil nanofluids

Multi objective optimization via RSM is a graphical illustration that validate the optimal values of the more than one manipulated variables that minimize or maximize the response variables and demonstrates the relationship of manipulated variables and response variables. This strategy is also essential to observe the sensitivity of specific corresponding to the changes in the independent variables. The benefits of employing RSM is to manipulate input constraints accordingly with the aim to enhance the specific response [26,45].

The previous sections stated the increase in temperature and volume concentration enhances the thermal conductivity properties of polyaniline-palm oil nanofluids. Density and viscosity exhibit contradict trend with the thermal conductivity properties, which both properties reported falling trend with respect to temperature, but increases with volume concentration of polyaniline nanofibers. This research is aim to extract the best combination of density, viscosity and thermal conductivity of the studied nanofluids. The

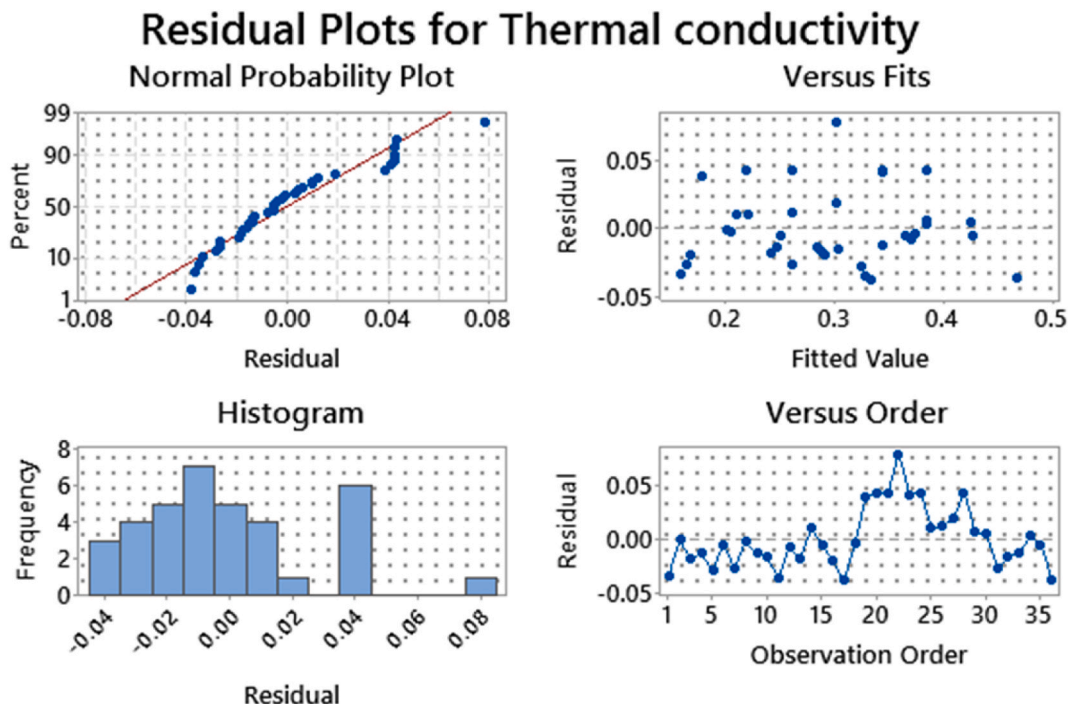


Fig. 18. Residual plot of thermal conductivity for polyaniline-palm oil nanofluids.

optimization plot of the thermal physical behavior of nanofluids presented in Fig. 19. The plot's optimum values for density, viscosity and thermal conductivity are 0.8878 g/mL, 25.8251 mPa s and 0.2877 W/mK respectively. The most significant parameters are 60 °C and 0.0347 vol%.

### 3.5. Economic analysis via price performance factor (PPF) evaluation

The research publications have exposed that the high cost of nanoadditives is one of the critical challenge in applying these technology in real life including engineering industrial application. There are many factors that give impact to high cost of nano-additives including; high cost of raw materials synthesize of nanoadditives, requirement for 99.99% purity of nanoadditives, advanced technology instruments and expensive procedures for synthesize of nanoadditives and limited fabrication of nanoadditives due to special approaches during production procedures [46–48]. When the expense for production of nanoadditives is high, the formulation of nanofluids for heat transfer application becomes a very expensive as well. US Research Nanomaterials in 2017 exposed the cost of formulated nanofluids in order to appropriately evaluate the full budgets and advantages of nanofluid system.

In Fig. 20, the relative thermal conductivity of polyaniline-pam oil nanofluids compared with preparation expenses of nanofluids at different volume concentration of nanoadditives and temperature. As it is known, the price of nanofluids found to be increased with volume concentration of nanoadditives as shown in Fig. 20 for all studied temperature. Fig. 20(a) presents relative thermal conductivity of polyaniline-palm oil nanofluids at different volume concentration at 30 °C. The relative thermal conductivity found to be increase with higher dispersion of polyaniline nanofibers due to the higher effect of Brownian motion in the nanofluid system. However, the relative thermal conductivity of nanofluids at temperature of 40, 50 and 60 °C in Fig. 20(b–d) found to be slightly increase with respect to volume concentration of nanoadditives as no clear significant increment obtained from the plotted graph. Theoretically, the cheaper expense of formulated nanofluids with more enhancement in heat transfer behavior are the more cost-effective nanofluids. This can conclude that the studied nanofluids are less economical as the enhancement of the thermal conductivity behavior is low as compared to the price of the nanofluids.

The economic analysis of the polyaniline-palm oil at the studied parameters was further extended via the calculation of price performance factor as displayed in Fig. 21. The PPF value found to be decrease with volume concentration of nanoadditives. Similar

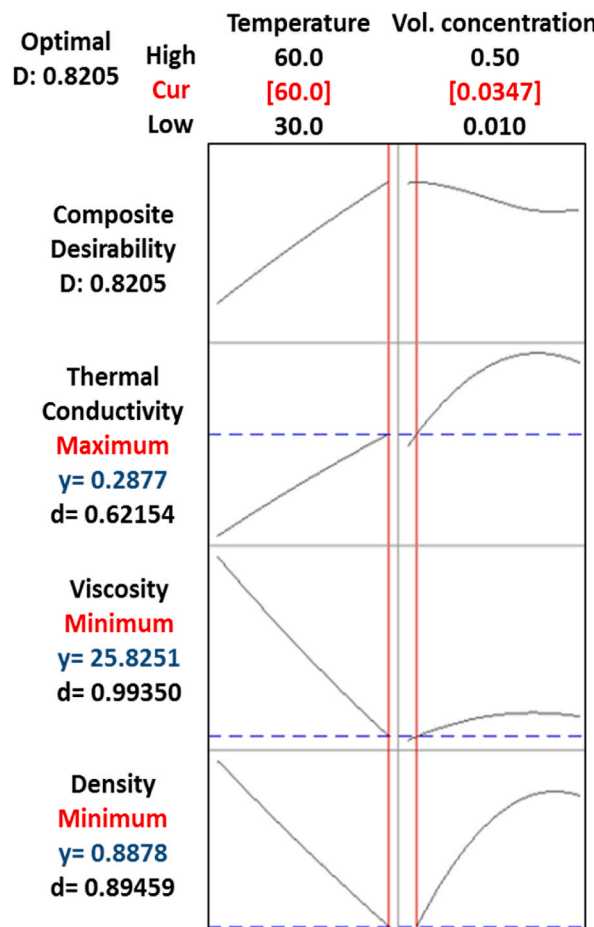


Fig. 19. Optimization plot of the thermal physical properties of polyaniline-palm oil nanofluids.

trend reported for all the plotted graph of PPF vs volume concentration of at different temperature, concluded that the polyaniline-palm oil nanofluids at studied parameters are not necessarily more economical. More enhancement of thermal conductivity properties required to improve the PPF in order to make it reliable in thermal storage application industries. The experiments carried out in the laboratory by researchers unveiled that various factors have an impact on the heat transfer characteristics of nanofluids. These factors include the size of particles, the material of the particles, the shape of nanoparticles, the amount of nanoadditives in the mixture, and the temperature. It was also determined that the enhancement of heat transfer can be attributed to the concentration of nanoadditives and the specific classes of nanoparticles. Additionally, the stability of nanofluid is a key parameter for a thermal system's consistent functioning at designed capacity. Dispersion stability is a crucial issue in nanofluid study because unstable system will eliminate all the benefits of the formulated suspension. The major challenge in formulation of homogeneous nanofluids is a strong van der Waals forces between nanoadditives especially when nanofluids serve as coolant for thermal transfer purposes [49,50]. The main challenge in dispersion stability of nanofluids system can be overcome by various strategy, as explored by researchers. They recommended to apply powerful forces on the agglomerated nanoadditives as one of the approaches to enhance dispersion stability of nanofluids system. For example, high frequency of probe sonicator, ultrasonic bath, ball milling and other approach of physical homogenizer can be applied to break down the clustered nanoadditives [51,52]. Other than that, further research can be carried out using various other conducting polymers such as polypyrrole and polythiophene to replace the polyaniline. The newly formulated class of nanofluids can subsequently undergo a properties investigation by varying their composition to assess their potential as additives within the nanofluid system. From the obtained report, we can conclude that this kind of analysis is necessary to figure out the economic status of the formulated nanofluids with the aim to provide a guideline for future research to alter and modify other parameters for formulation of nanofluids such as morphology of nanoadditives, dimension of nanoadditives and dispersion of surfactant to enhance stability towards a better properties of nanofluid system [53–55].

#### 4. Conclusions

The present research work highlights the formulation of polyaniline-palm oil nanofluids and to investigate the density, viscosity and thermal conductivity properties with volume concentration of 0.01–0.5 vol% and temperature of 30–60 °C. A mathematical model was developed and proposed to predict the formulated nanofluid's optimal thermophysical properties and validation. The summarized findings and discussion as follows:

- The density of all nanofluids increased with volume concentration of nanoadditives but decrease with temperature

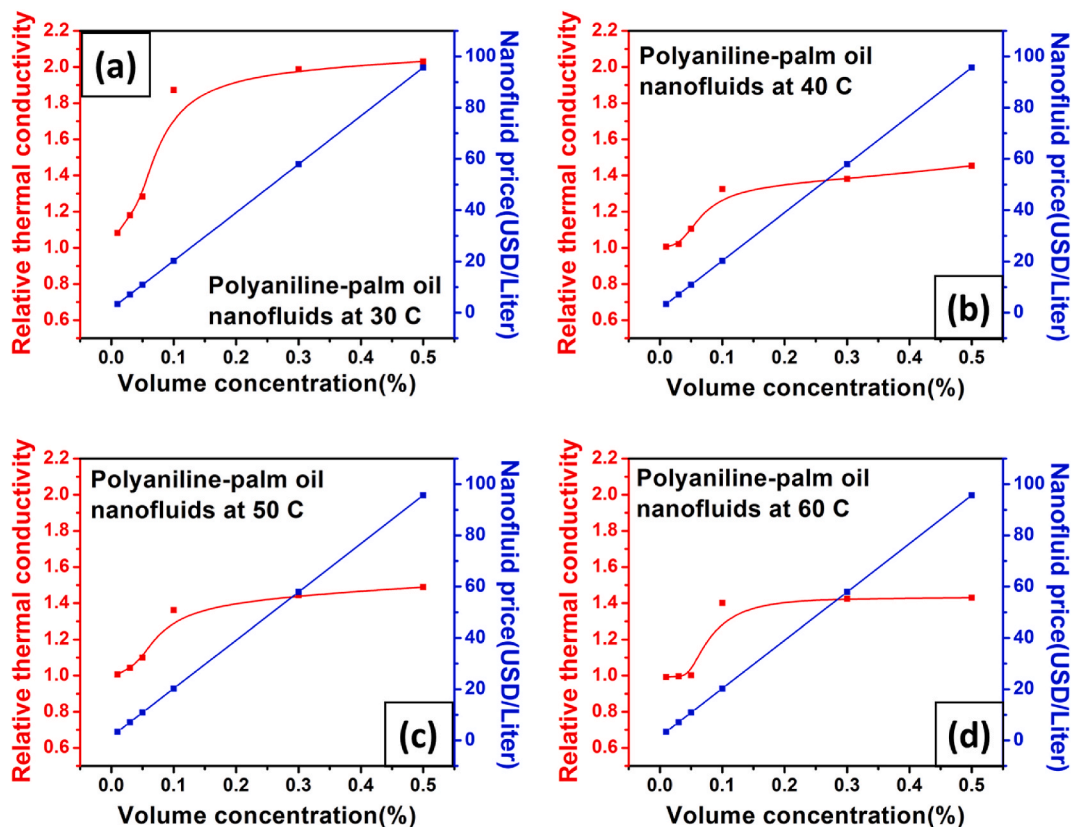


Fig. 20. Relative thermal conductivity and price of polyaniline-palm oil nanofluids at different temperature, (a) 30 °C, (b) 40 °C, (c) 50 °C and (d) 60 °C.

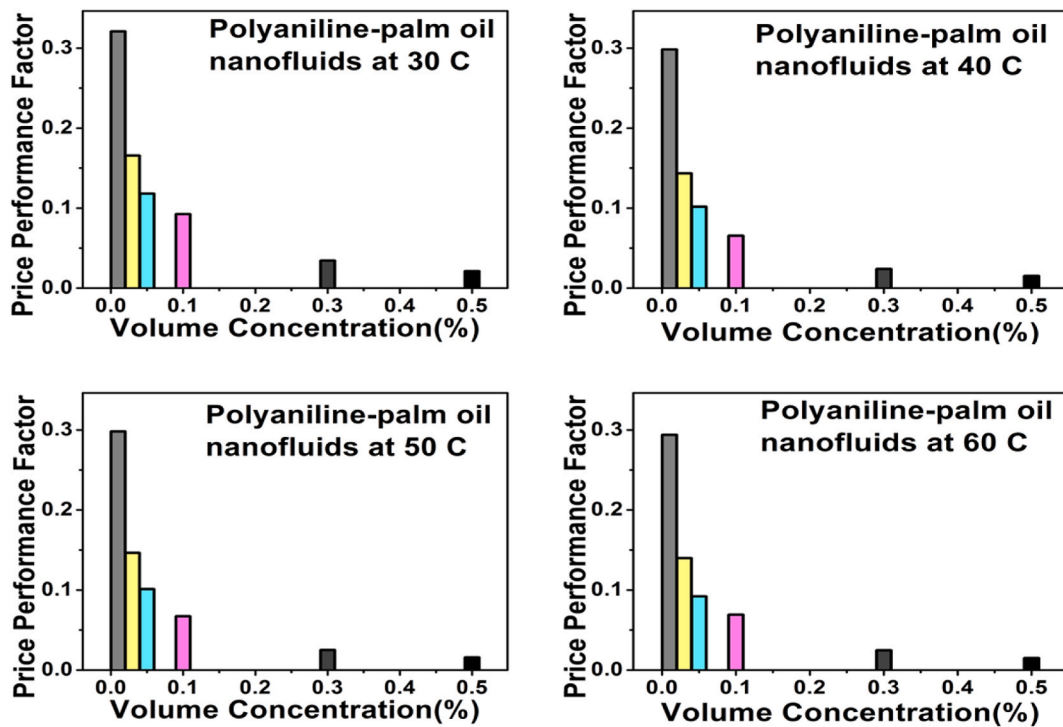


Fig. 21. Price performance factor for polyaniline-palm oil nanofluids at different temperature.

- Nanofluids' viscosity was found to increase correspond to amount of nanoadditives dispersed in palm oil, but their viscosity were diminished at high temperature.
- From thermal conductivity measurement, the thermal conductivity was seen to improve with the increase in volume concentration and temperature and was found to be at its maximum for 0.5% volume concentration and 60 °C between all prepared nanofluids.
- RSM approach strategy has successfully employed for predicting the density, viscosity, and thermal thermophysical properties of nanofluids as a function of volume percentage of nanoadditives and temperature conductivity of nanofluids.
- The formation of 45° angle line in the middle of the predicted vs actual data graph with acceptable  $R^2$  value of 94.43% for density model, 99.43% for viscosity model, and 94.18% for the thermal conductivity model showing an excellent agreement of both predicted and actual data and verified the reliability of the generated regression equation for response prediction. Optimal density, viscosity and thermal conductivity of polyaniline-palm oil nanofluids found to be 0.8878 g/mL, 25.8251 mPa s and 0.2877 W/mK respectively with the critical parameters for temperature and volume concentration of polyaniline are 60 °C and 0.0347 vol% respectively.
- This inclusive employment of multiple input parameters ensures the precise prediction of nanofluid density, viscosity and thermal conductivity and permits experimental scrutiny of the nanofluids composed of polyaniline nanofibers disprsd in palm oil base fluids.
- Furthermore, the model devised will be applied to ascertain the optimal input parameters for either minimizing or maximizing of these studied properties
- From the PPF evaluation, the polyaniline-palm oil nanofluids at studied parameters are not practically economical as the plotted PPF graph shows a decrement of the PPF value with respect to volume concentration.

#### Declaration of competing interest

The authors declare that they have no known competing financial interests or personal relationships that could have appeared to influence the work reported in this paper.

#### Data availability

No data was used for the research described in the article.

#### Acknowledgement

This work was supported by the Ministry of Higher Education of Malaysia through the HICoE grant (2022001HICOE), Dato' Low Tuck Kwong International Energy Transition Grant (202203004ETG), AAIBE Chair of Renewable Energy (202202KETTTHA) as well as

Tenaga Nasional Berhad (TNB) and UNITEN through the BOLD Refresh Publication Fund under the project code of J510050002-IC-6 BOLDREFRESH2025-Centre of Excellence.

## Appendix A. Supplementary data

Supplementary data to this article can be found online at <https://doi.org/10.1016/j.csite.2023.103673>.

### List of symbols

|               |  |
|---------------|--|
| $\varnothing$ | Volume concentration %                 |
| $bf$          | Base fluid                             |
| $k$           | Thermal conductivity (W/mK)            |
| $M$           | Molarity                               |
| $n$           | Number of variables                    |
| $nf$          | Nanofluids                             |
| $p$           | Particles                              |
| $PPF$         | Price Performance Factor               |
| $RTC$         | Relative thermal conductivity          |
| $T$           | Temperature (°C)                       |
| $w$           | Weight(g)                              |
| $Y$           | Predicted response                     |
| $\varepsilon$ | Residual associated to the experiments |
| $\mu$         | Viscosity (mPa.s)                      |
| $\rho$        | Density(g/mL)                          |
| $\beta_0$     | Intercept                              |
| $\beta_i$     | First model of linear parameters       |
| $\beta_{ii}$  | Second-order (quadratic) coefficient   |
| $\beta_{ij}$  | Coefficient of an interaction effect   |

### References

- [1] F.L. Rashid, A. Hashim, Recent review on nanofluid/nanocomposites for solar energy storage, *International Journal of Scientific Research and Engineering Development* 3 (4) (2020) 780–789.
- [2] M.M. Azim, et al., Recent progress in emerging hybrid nanomaterials towards the energy storage and heat transfer applications: a review, *J. Mol. Liq.* 360 (2022), 119443.
- [3] Z.A. Alrowaili, et al., Investigation of the effect of hybrid CuO-Cu/water nanofluid on the solar thermal energy storage system, *J. Energy Storage* 50 (2022), 104675.
- [4] J. Li, et al., Nanofluid research and applications: a review, *Int. Commun. Heat Mass Tran.* 127 (2021), 105543.
- [5] A. Sofiah, et al., Immense impact from small particles: review on stability and thermophysical properties of nanofluids, *Sustain. Energy Technol. Assessments* 48 (2021), 101635.
- [6] S. Chakraborty, P.K. Panigrahi, Stability of nanofluid: a review, *Appl. Therm. Eng.* 174 (2020), 115259.
- [7] M. Muneeshwaran, et al., Role of hybrid-nanofluid in heat transfer enhancement—A review, *Int. Commun. Heat Mass Tran.* 125 (2021), 105341.
- [8] M. Bhatti, et al., Swimming of Gyrotactic Microorganism in MHD Williamson nanofluid flow between rotating circular plates embedded in porous medium: application of thermal energy storage, *J. Energy Storage* 45 (2022), 103511.
- [9] G.B. Abdelaziz, et al., Performance enhancement of tubular solar still using nano-enhanced energy storage material integrated with v-corrugated aluminum basin, wick, and nanofluid, *J. Energy Storage* 41 (2021), 102933.
- [10] M.A.M. Akanda, D. Shin, A synthesis parameter of molten salt nanofluids for solar thermal energy storage applications, *J. Energy Storage* 60 (2023), 106608.
- [11] H. Nabi, M. Gholinia, D. Ganji, Employing the (SWCNTs-MWCNTs)/H<sub>2</sub>O nanofluid and topology structures on the microchannel heatsink for energy storage: a thermal case study, *Case Stud. Therm. Eng.* 42 (2023), 102697.
- [12] M.M. Mohamed, N.H. Mahmoud, M.A. Farahat, Energy storage system with flat plate solar collector and water-ZnO nanofluid, *Sol. Energy* 202 (2020) 25–31.
- [13] M. Bezaatpour, H. Rostamzadeh, Simultaneous energy storage enhancement and pressure drop reduction in flat plate solar collectors using rotary pipes with nanofluid, *Energy Build.* 239 (2021), 110855.
- [14] M. Ding, C. Liu, Z. Rao, Experimental investigation on heat transfer characteristic of TiO<sub>2</sub>-H<sub>2</sub>O nanofluid in microchannel for thermal energy storage, *Appl. Therm. Eng.* 160 (2019), 114024.
- [15] Y. Gao, et al., Thermal conductivity and stability of novel aqueous graphene oxide–Al<sub>2</sub>O<sub>3</sub> hybrid nanofluids for cold energy storage, *Appl. Sci.* 10 (17) (2020) 5768.
- [16] M. George, et al., Long-term thermophysical behavior of paraffin wax and paraffin wax/polyaniline (PANI) composite phase change materials, *J. Energy Storage* 31 (2020), 101568.
- [17] A. Sofiah, et al., A comparative experimental study on the physical behavior of mono and hybrid RBD palm olein based nanofluids using CuO nanoparticles and PANI nanofibers, *Int. Commun. Heat Mass Tran.* 120 (2021), 105006.
- [18] A. Sofiah, et al., Copper (II) oxide nanoparticles as additives in RBD palm olein: experimental analysis and mathematical modelling, *J. Mol. Liq.* 363 (2022), 119892.
- [19] A. Sofiah, et al., An experimental study on characterization and properties of eco-friendly nanolubricant containing polyaniline (PANI) nanotubes blended in RBD palm olein oil, *J. Therm. Anal. Calorim.* 145 (2021) 2967–2981.
- [20] B. Bhanvase, S. Sonawane, Ultrasound assisted in situ emulsion polymerization for polymer nanocomposite: a review, *Chem. Eng. Process: Process Intensif.* 85 (2014) 86–107.

- [21] M. Osama, et al., Physical properties optimization of POME-groundnut-naphthenic based graphene nanolubricant using response surface methodology, *J. Clean. Prod.* 193 (2018) 277–289.
- [22] T. Woma, et al., The base oil used for the formulation of most lubricants is environmentally hostile mineral oil and 30% of lubricants consumed ends up in the ecosystem. However, mineral oil reserve is depleting and the environmental concern about the damaging impact of mineral oil is growing, *Tribol. Online* 14 (2019) 60–70.
- [23] A. Sofiah, et al., Copper oxide/polyaniline nanocomposites-blended in palm oil hybrid nanofluid: thermophysical behavior evaluation, *J. Mol. Liq.* 375 (2023), 121303.
- [24] S. Syahrullail, et al., Experimental evaluation of palm oil as lubricant in cold forward extrusion process, *Int. J. Mech. Sci.* 53 (7) (2011) 549–555.
- [25] O. Mahian, et al., Recent advances in modeling and simulation of nanofluid flows-Part I: fundamentals and theory, *Phys. Rep.* 790 (2019) 1–48.
- [26] Y.-M. Chu, et al., Examining rheological behavior of MWCNT-TiO<sub>2</sub>/5W40 hybrid nanofluid based on experiments and RSM/ANN modeling, *J. Mol. Liq.* 333 (2021), 115969.
- [27] A. Hemmati-Sarapardeh, et al., On the evaluation of the viscosity of nanofluid systems: modeling and data assessment, *Renew. Sustain. Energy Rev.* 81 (2018) 313–329.
- [28] H.S. Pali, et al., Enhancement of combustion characteristics of waste cooking oil biodiesel using TiO<sub>2</sub> nanofluid blends through RSM, *Fuel* 331 (2023), 125681.
- [29] A. Aa, et al., Comparison of the Properties of Palm Oil and Palm Kerneloil Biodiesel in Relation to the Degree of Unsaturation of Their Oil Feedstocks, 2016.
- [30] L. Samylingam, et al., Thermal and energy performance improvement of hybrid PV/T system by using olein palm oil with MXene as a new class of heat transfer fluid, *Sol. Energy Mater. Sol. Cell.* 218 (2020), 110754.
- [31] M.H. Esfe, S. Alidoust, D. Toghraie, Comparison of the thermal conductivity of hybrid nanofluids with a specific proportion ratio of MWCNT and TiO<sub>2</sub> nanoparticles based on the price performance factor, *Mater. Today Commun.* 34 (2023), 105411.
- [32] A. Alirezaie, et al., Price-performance evaluation of thermal conductivity enhancement of nanofluids with different particle sizes, *Appl. Therm. Eng.* 128 (2018) 373–380.
- [33] M.H. Esfe, et al., Thermal conductivity of MWCNT-TiO<sub>2</sub>/Water-EG hybrid nanofluids: calculating the price performance factor (PPF) using statistical and experimental methods (RSM), *Case Stud. Therm. Eng.* 48 (2023), 103094.
- [34] A. Zainoodin, et al., Optimization of a porous carbon nanofiber layer for the membrane electrode assembly in DMFC, *Energy Convers. Manag.* 101 (2015) 525–531.
- [35] A. Afshari, et al., Experimental investigation of rheological behavior of the hybrid nanofluid of MWCNT–alumina/water (80%)–ethylene-glycol (20%), *J. Therm. Anal. Calorim.* 132 (2) (2018) 1001–1015.
- [36] S. Khaliq, Z. Abbas, A theoretical analysis of roll-over-web coating assessment of viscous nanofluid containing Cu-water nanoparticles, *J. Plast. Film Sheeting* 36 (1) (2020) 55–75.
- [37] S.S. Sanukrishna, M. Jose Prakash, Experimental studies on thermal and rheological behaviour of TiO<sub>2</sub>-PAG nanolubricant for refrigeration system, *Int. J. Refrig.* 86 (2018) 356–372.
- [38] S. Saedodin, M.H. Kashefi, Z. Bahrami, Experimental study on the rheological behavior of nanolubricant-containing MCM-41 nanoparticles with viscosity measurement, *J. Therm. Anal. Calorim.* 137 (5) (2019) 1499–1511.
- [39] W. Azmi, et al., Effects of working temperature on thermo-physical properties and forced convection heat transfer of TiO<sub>2</sub> nanofluids in water–Ethylene glycol mixture, *Appl. Therm. Eng.* 106 (2016) 1190–1199.
- [40] R.M. Abumandour, et al., Peristaltic thrusting of a thermal-viscosity nanofluid through a resilient vertical pipe, *Z. Naturforsch.* 75 (8) (2020) 727–738.
- [41] R. Lenin, P.A. Joy, C. Bera, A review of the recent progress on thermal conductivity of nanofluid, *J. Mol. Liq.* 338 (2021), 116929.
- [42] R. Bakhtiari, et al., Preparation of stable TiO<sub>2</sub>-Graphene/Water hybrid nanofluids and development of a new correlation for thermal conductivity, *Powder Technol.* 385 (2021) 466–477.
- [43] H. Younes, et al., Nanofluids: key parameters to enhance thermal conductivity and its applications, *Appl. Therm. Eng.* 207 (2022), 118202.
- [44] M. Pavia, et al., A critical review on thermal conductivity enhancement of graphene-based nanofluids, *Adv. Colloid Interface Sci.* 294 (2021), 102452.
- [45] C.T. Yaw, et al., An approach for the optimization of thermal conductivity and viscosity of hybrid (graphene nanoplatelets, GNPs: cellulose nanocrystal, CNC) nanofluids using response surface methodology (RSM), *Nanomaterials* 13 (10) (2023) 1596.
- [46] B.V. Balakin, P.G. Struchalin, Eco-friendly and low-cost nanofluid for direct absorption solar collectors, *Mater. Lett.* 330 (2023), 133323.
- [47] M. Abubakr, et al., An intuitive framework for optimizing energetic and exergetic performances of parabolic trough solar collectors operating with nanofluids, *Renew. Energy* 157 (2020) 130–149.
- [48] S.M.S. Hosseini, M. Mirzaei, Assessment of the colloidal montmorillonite dispersion as a low-cost and eco-friendly nanofluid for improving thermal performance of plate heat exchanger, *SN Appl. Sci.* 2 (10) (2020) 1719.
- [49] S. Mukherjee, S. Paria, Preparation and stability of nanofluids-a review, *IOSR J. Mech. Civ. Eng.* 9 (2) (2013) 63–69.
- [50] S. Sharma, S.M. Gupta, Preparation and evaluation of stable nanofluids for heat transfer application: a review, *Exp. Therm. Fluid Sci.* 79 (2016) 202–212.
- [51] Y. Hwang, et al., Production and dispersion stability of nanoparticles in nanofluids, *Powder Technol.* 186 (2) (2008) 145–153.
- [52] P. Thakur, et al., Nanofluids-based delivery system, encapsulation of nanoparticles for stability to make stable nanofluids, in: *Encapsulation of Active Molecules and Their Delivery System*, Elsevier, 2020, pp. 141–152.
- [53] B. Bakthavatchalam, et al., Comprehensive study on nanofluid and ionanofluid for heat transfer enhancement: a review on current and future perspective, *J. Mol. Liq.* 305 (2020), 112787.
- [54] B. Mehta, et al., Synthesis, Stability, Thermophysical Properties and Heat Transfer Applications of Nanofluid–A Review, *Journal of Molecular Liquids*, 2022, 120034.
- [55] H. Adun, D. Kavaz, M. Dagbasi, Review of ternary hybrid nanofluid: synthesis, stability, thermophysical properties, heat transfer applications, and environmental effects, *J. Clean. Prod.* 328 (2021), 129525.